Available online at www.sciencedirect.com
ScienceDirect
Journal of Catalysis 244 (2006) 163–168
JOURNAL OF CATALYSIS
www.elsevier.com/locate/jcat

Catalytic activity of Brønsted acid sites in zeolites: Intrinsic activity, rate-limiting step, and influence of the local structure of the acid sites

Bin Xu [a], Carsten Sievers [b], Suk Bong Hong [c], Roel Prins [a], Jeroen A. van Bokhoven [a,*]

[a] *Institute for Chemical and Bioengineering, ETH Zurich, 8093 Zurich, Switzerland*
[b] *Department of Chemistry, TU München, D-85747 Garching, Germany*
[c] *Division of Applied Chemistry and Biotechnology, Hanbat National University, Taejon 305-719, South Korea*

Received 2 June 2006; revised 7 August 2006; accepted 30 August 2006

Available online 9 October 2006

Abstract

The catalytic activity of Brønsted acid sites in zeolites was studied by the monomolecular conversion of propane over zeolites with varying framework topologies and Si/Al ratios. The rates and apparent activation energies of cracking and dehydrogenation were determined. The activity of the Brønsted acid sites depends on the rate-limiting step of the reaction. In the cracking reaction, the protonation of the alkane is the rate-limiting step, and the heat of reactant adsorption dominates the differences in the observed activity. The similar intrinsic activities over the different zeolites show that the ability of zeolitic Brønsted acid sites to transfer a proton to an alkane does not vary significantly, suggesting that the acid sites that participate in the reaction have very similar strengths. In the dehydrogenation reaction, the rate-limiting step is the desorption of the alkoxide species. The rate is determined by the stability of the alkoxide species, which is influenced by the local geometric and electronic structure of the Brønsted acid site and is affected by zeolite structure and Si/Al ratio. Implications of these conclusions are related to other reactions, such as catalytic cracking and alkylation.

Keywords: Alkane cracking; Alkane dehydrogenation; Monomolecular cracking; Zeolite characterization; Alkoxide species; Heat of adsorption; Intrinsic activity

1. Introduction

Acid-catalyzed hydrocarbon transformations, such as cracking, isomerization, and alkylation, are very important reactions in the petrochemical industry. Zeolites are used in several of these reactions, as well as in many reactions in the production of fine chemicals. The zeolitic Brønsted acid sites are the active species in many of these reactions [1,2]. Therefore, characterizing the Brønsted acid sites in zeolites and determining the structure–activity relationship are of fundamental importance in understanding and improving zeolites for use as catalysts.

Alkanes can be activated by two mechanisms, depending on the reaction conditions [3–5]: a monomolecular mechanism and a bimolecular mechanism. In the monomolecular mechanism, an alkane is protonated by a Brønsted acid site [6–10] to form a five-coordinated carbon atom. This carbonium ion may undergo cracking to yield an alkane and an alkene, regenerating the acid site, or it may dehydrogenate to yield H_2 and an alkoxide species [11]. Desorption of the alkoxide yields an olefin and regenerates the acid site. Alternatively, alkoxides may initiate bimolecular reactions. Scheme 1 shows the monomolecular reactions of propane. Reaction (1) represents cracking, with a rate-determining step of protonation [12]; reaction (2) represents dehydrogenation, with a rate-determining step of olefin desorption [13]. Low reactant pressure, low conversion, and high temperature favor the monomolecular reaction, and the resulting product distribution is simple. In the bimolecular mechanism, however, an alkane is activated by hydride transfer between the alkane and the adsorbed alkoxide species [9,14–21]. This reaction may be followed by β-scission or isomerization [3,4,22]. The alkoxide species can be formed in the monomolecular dehydrogenation reaction or by adsorption of olefins present in the reactant feed or formed early in the reactor. The rate-limiting step in the bimolecular mechanism is hydride transfer after initial formation of the alkoxide

* Corresponding author.
E-mail address: j.a.vanbokhoven@chem.ethz.ch (J.A. van Bokhoven).

0021-9517/$ – see front matter
doi:10.1016/j.jcat.2006.08.022

$$C_3H_8 + H^{+-}OZ \xrightarrow{\text{r.l.s.}} [C_3H_9]^{+-}OZ \rightarrow CH_4 + C_2H_4 + H^{+-}OZ \quad (1)$$

$$C_3H_8 + H^{+-}OZ \rightarrow [C_3H_9]^{+-}OZ \rightarrow H_2 + C_3H_7\text{–}OZ \quad (2)$$
$$\downarrow \text{r.l.s.}$$
$$C_3H_6 + H^{+-}OZ$$

Scheme 1. Propane monomolecular reaction (r.l.s. = rate limiting step).

species [11]. High reactant pressure, high conversion, and low temperature favor the reactions in the bimolecular mechanism, and, due to the dimerization, oligomerization, isomerization, and β-scission reactions, the product distribution is complicated.

Monomolecular conversion of small alkanes is a good reaction for characterizing zeolites and establishing the relationship between their structure and catalytic activity. The reactants are physisorbed in the pores of the zeolites and at high temperature are activated through proton transfer from the Brønsted acid sites. Because the rate-limiting step of monomolecular cracking is the protonation of the alkane, this reaction is an acid–base reaction between the zeolite and the alkane. Therefore, its intrinsic rate is a measure of zeolitic acidity. The intrinsic activation energy (E_{int}) equals the apparent activation energy (E_{app}) minus the heat of reactant adsorption (ΔH_{ads}) [23] as follows:

$$E_{\text{int}} = E_{\text{app}} - \Delta H_{\text{ads}}. \quad (3)$$

In contrast, the rate-limiting step in the dehydrogenation reaction is desorption of the olefins [13]. The stability of the alkoxide species depends strongly on the local neighborhood of the Brønsted acid site [24], and the intrinsic reaction parameters of the dehydrogenation reflect the stability of the alkoxide species.

Several studies have used the monomolecular cracking of hexane to characterize the Brønsted acid sites of different zeolites [25–27]. The results show that different zeolites have different activities. These differences were interpreted as being due to the different heats of reactant adsorption (ΔH_{ads}) [25,27] and to the different acid strengths of the Brønsted acid sites in various zeolites [26]. Here we report the intrinsic activity of the Brønsted acid sites and the influence of the local structure of the Brønsted acid sites by determining the cracking and dehydrogenation pathways of the conversion of propane. The influence of zeolite type and framework Si/Al ratio were studied.

2. Experimental

2.1. Catalyst preparation

Four different structure types (MFI, MOR, Beta, and FAU) of zeolites were used. Table 1 lists the samples and their physical properties. ZSM5 was prepared by hydrothermal synthesis [28]. As-made ZSM5 was calcined in air at 823 K for 5 h to remove the structure-directing agent and then converted to the NH_4 form by triple ion exchange with 1 M NH_4NO_3 solutions at 353 K. MOR samples with Si/Al = 4.9, 9.9, and 16.7 in the Na form were obtained from Tosoh. Three Beta samples with Si/Al ratios of 10.5, 27, and 110 were as described previously [29]. A NaY with Si/Al = 2.6 was obtained from BP Amoco. All of these samples were converted to the NH_4-form following procedures identical to those for NH_4ZSM5 preparation. The residual Na content of each material determined by atomic absorption spectroscopy (AAS) was about 0.05 wt%.

Table 1
Properties of zeolite samples

Sample	Si/Al ratio[a]	BET surface area[b] (m^2/g)	Micropore volume[b] (cm^3/g)	Brønsted acid sites[c] (mmol/g)
ZSM5	39	370	0.13	0.42
4.9MOR	4.9	380	0.15	1.39
9.9MOR	9.9	510	0.20	0.90
16.7MOR	16.7	490	0.19	0.67
10.5Beta	10.5	490	0.17	0.90
27Beta	27	490	0.18	0.51
110Beta	110	370	0.14	0.14
Y	2.6	810	0.32	1.95

[a] Determined by AAS.
[b] Determined by N_2 physisorption.
[c] Determined by the decomposition of *i*-propylamine.

2.2. Characterization

N_2 physisorption measurements were performed at 77 K on a Micromeritics ASAP 2000 apparatus. Before the measurements, all samples were degassed overnight at 723 K. The surface area was determined by the BET method, and the micropore volume was determined from the intercept of the linear part of the *t*-plot. ^{27}Al MAS NMR measurements were performed at 104.287 MHz on a Bruker Avance AMX-400 spectrometer at a spinning rate of 12 kHz using a 4-mm probe head. A single pulse length of $\pi/6$ was used.

The number of Brønsted acid sites was determined with decomposition of *i*-propylamine [30]. In laboratory-constructed equipment, approximately 20–40 mg of sample was activated at $P < 10^{-4}$ Pa overnight by heating to 723 K at a ramp rate of 2 K/min. The sample was exposed to *i*-propylamine at 473 K for 2 h, then cooled to room temperature and evacuated for ∼2 h to remove the physically adsorbed *i*-propylamine. The decomposition experiment was performed at a heating rate of 10 K/min and a flow of 20 mL/min Ar in a Mettler Toledo TGA/SDTA851e instrument for thermogravimetric analysis (TGA). The amount of decomposed *i*-propylamine was obtained from the mass changes in the TGA curve between 573 and 650 K.

The heat of adsorption was measured with a modified Setaram TG-DSC 111 instrument with a baratron pressure transducer. The sample was pressed into pellets, and 10–15 mg of the sample was placed into a quartz crucible. The sample was activated for 1 h at $P < 10^{-4}$ Pa and at 823 K at a heating ramp of 10 K/min. After activation, alkanes were added in pulses at 343 K. The system was allowed to equilibrate, as confirmed by observation of the sample weight, heat flow, and pressure. The system was considered in equilibrium once it was observed to

be stable for several minutes. The differential heats of adsorption were measured using a calorimeter.

2.3. Propane monomolecular conversion

The catalytic reaction was performed in a setup with six parallel-flow tubular quartz reactors, with 10% propane (10 kPa) in argon at 675 to 875 K and 100 kPa total pressure. Propene was not detected in the feed. The flow rates varied from 5 to 50 mL/min, and the catalyst weight varied from 50 to 100 mg. Before the reaction, the catalysts were activated in the reactor in 10% oxygen in argon at 878 K for 1 h at a heating ramp of 2 K/min. Lower pretreatment temperatures did not affect the rates, indicating that the high pretreatment temperature did not alter the structure that influenced the catalytic results. The products were analyzed in the effluent gas stream with an on-line gas chromatograph (Agilent 3000 MicroGC). The MicroGC comprises three self-contained modules, each consisting of an injector, column, flow control valve, and a thermal conductivity detector, the latter of which can be used to analyze natural gas and refinery gases. Three columns were used: MolSieve 5A, PLOT U, and Alumina PLOT.

The apparent activation energies were determined from the slopes of the Arrhenius plots. The reproducibility was better than 3 kJ/mol, obtained by averaging three measurements on newly prepared catalysts. The reaction conditions were chosen so that the molar ratios of C_1 and $C_2^=$ and of H_2 and $C_3^=$ were unity; no hydrocarbons with more than three atoms were detected. Conversion was kept below 5%. Thus, hydride transfer and secondary cracking did not occur. After the reaction, all of the catalysts were white.

3. Results

Fig. 1 shows the ^{27}Al MAS NMR spectra of the zeolite samples. For all of the samples, only a single peak at around 60 ppm was observed, assigned to a tetrahedrally coordinated framework Al. The positions of the peaks of the samples differed because of the varying average Al–O–Si angles in the structures. None of the samples showed an octahedral coordination typical of nonframework Al.

The Arrhenius plots of the monomolecular conversion of propane over the MOR and Beta samples with different Si/Al ratios are shown in Figs. 2 and 3, respectively. For both the MOR and Beta zeolites, the Arrhenius plots of the cracking reaction were parallel, but the slopes of the dehydrogenation reaction increased with increasing Si/Al ratio. Table 2 gives the apparent activation energies, reaction rates, and selectivities of the two reaction pathways of all samples at 823 K. The table also gives the turnover frequencies based on the number of Brønsted acid sites determined by *i*-propylamine decomposition (Table 1) and the rates per gram of cracking of propane. The activities per Brønsted acid site decreased in the order ZSM5 ⩾ MOR > Beta > FAU. The Si/Al ratios of MOR and Beta affected the activities per Brønsted acid site at most by a factor of two, which is smaller than the difference in zeolite structure types. The different rates per Brønsted acid site are reflected in variations in the activation energies, which decreased in the opposite order: FAU > Beta > MOR ⩾ ZSM5.

The rates of dehydrogenation per Brønsted acid site decreased in the order ZSM5 ⩾ MOR > Beta > FAU. The Si/Al ratio did not affect the rates more than a factor of two. Unlike

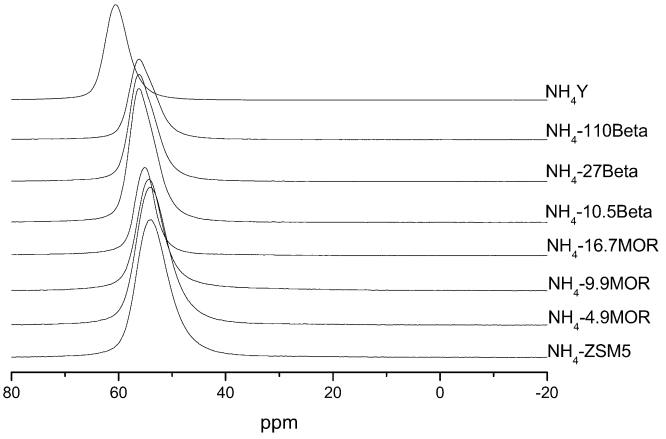

Fig. 1. ^{27}Al MAS NMR spectra of NH_4-zeolites.

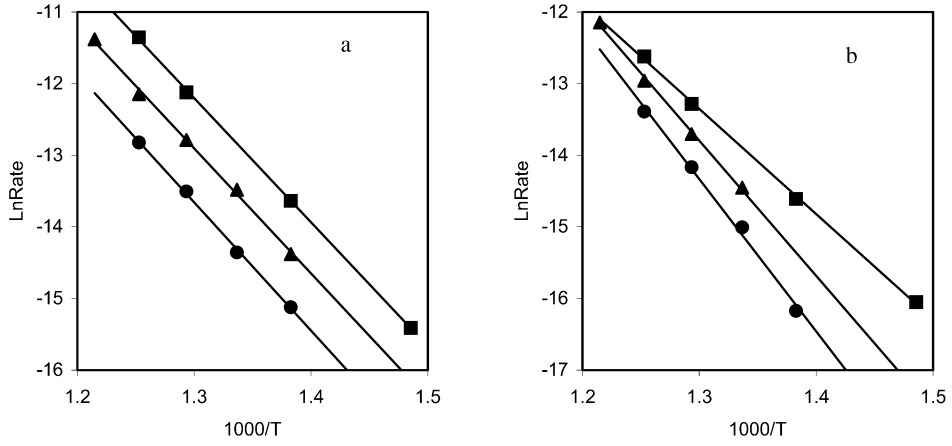

Fig. 2. Arrhenius plots of monomolecular conversion of propane over MOR samples: (a) cracking and (b) dehydrogenation: 4.9MOR (■), 9.9MOR (▲), and 16.7MOR (●).

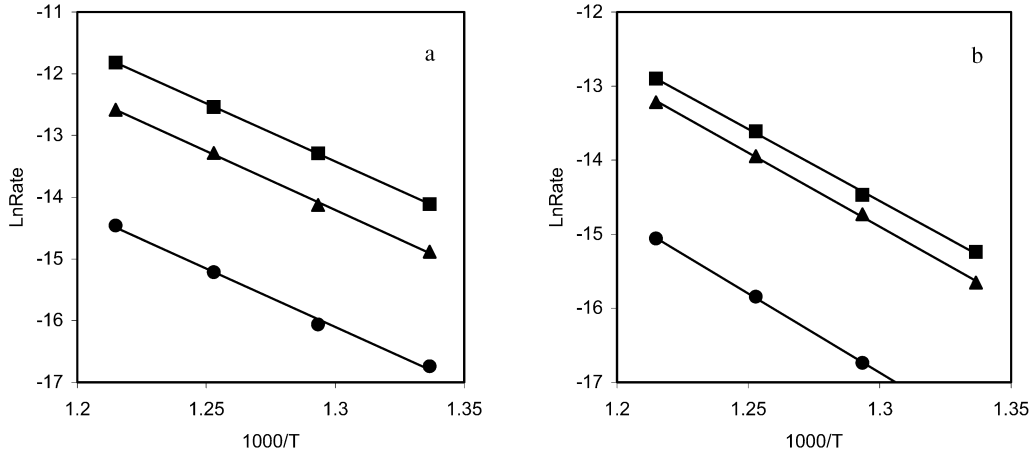

Fig. 3. Arrhenius plots of monomolecular conversion of propane over Beta samples: (a) cracking and (b) dehydrogenation: 10.5Beta (■), 27Beta (▲), and 110Beta (●).

Table 2
Reaction rates and apparent activation energies of monomolecular conversion of propane over MOR and Beta zeolite samples

Sample	Rate cracking[a] $\times 10^{-6}$ (mol/(g s bar))	Rate cracking[b] $\times 10^{-6}$ (mol/(mmol s bar))	Rate dehydrogenation[a] $\times 10^{-6}$ (mol/(g s bar))	Rate dehydrogenation[b] $\times 10^{-6}$ (mol/(mmol s bar))	E_{app}^{cr} (kJ/mol)	E_{app}^{de} (kJ/mol)	$100 \times$ cr/(cr + de)[c]
ZSM5	9.9	23.6	5.0	11.9	147	157	66
4.9MOR	32	23.0	7.6	5.5	145	123	81
9.9MOR	20	22.2	8.3	9.2	145	134	71
16.7MOR	6.9	10.3	3.4	5.1	149	172	67
10.5Beta	6.2	6.9	3.0	3.3	157	161	67
27Beta	3.2	6.3	2.3	4.5	159	169	58
110Beta	0.5	3.6	0.4	2.8	156	178	56
Y	0.29	0.15	0.24	0.12	165	173	55

[a] Rate at 823 K per gram.
[b] Rate at 823 K per Brønsted acid site determined by the decomposition of *i*-propylamine.
[c] Selectivity to cracking in percentage at 823 K.

cracking, the activation energies of dehydrogenation of propane showed no trend with zeolite pore size. The activation energies significantly increased with Si/Al ratio for zeolites MOR and Beta. The selectivity to cracking decreased with increasing Si/Al ratio: 81, 71, and 67% for the MOR samples and 67, 58, and 56% for the Beta samples.

4. Discussion

4.1. Intrinsic activity per site: cracking

In protolytic cracking, alkane protonation is the rate-limiting step [13]. Because this involves the transfer of a proton to a weak base, the intrinsic activity of cracking is a means of measuring the acid strength of the Brønsted acid sites [1,31–34]. All zeolite samples used in this study have only tetrahedrally coordinated aluminium, as shown by ^{27}Al MAS NMR (Fig. 1), which is the framework Al that generates the Brønsted acid site. Thus, the catalytic results are not influenced by extra-framework Al or Lewis acid sites. However, not all tetrahedral Al contributes to active Brønsted acid sites [35,36]. To determine the TOF, we determined the number of active sites via decomposition of *i*-propylamine assuming that those sites participate in the reaction [30], which may be an approximation.

Different structure types of zeolites have distinctly different activities per gram in monomolecular cracking of propane. However, the activities per Brønsted acid site and the activation energies vary systematically with pore size; large pore zeolites showed lower activities per Brønsted acid site and higher activation energies (Table 2), in agreement with previous reports [25,27,34]. The Si/Al ratios in MOR and Beta had no effect on activation energy. Alkanes are physisorbed in the pores of a zeolite and the dominant interactions are the dispersion forces (the van der Waals interaction). The strength of the adsorption depends on the fit of alkane within the pore; the better the fit, the greater the heat of adsorption [37,38]. Activation of the alkane occurs through protonation at high temperature. The intrinsic activation energies were calculated using Tempkin's equation [Eq. (3)], and are reported in Table 3. The values were very close to those reported by Narbeshuber et al. for cracking of alkanes of various lengths on ZSM5 [12]. The intrinsic activation energies varied less than the apparent ones, and the heat of adsorption was the major parameter affecting the apparent activation energies. Previously, a compensation relation between the heat and entropy of adsorption over different zeolites was found [39]. In combination with the compensation relation for cracking [27], it was suggested that the acid strength of the catalysts is much less important than the adsorption term,

Table 3
Intrinsic activity of propane monomolecular cracking over zeolite samples

Samples	Pore structure		$\Delta H_{ads}^{C_3H_8}$ (kJ/mol)	E_{app}^{cr} (kJ/mol)	E_{int} (kJ/mol)
MFI	10 MR	5.1 × 5.5 Å 5.3 × 5.6 Å	−46	147	193
MOR	8 MR 12 MR	2.6 × 5.7 Å 6.5 × 7.0 Å	−41	145–149	186–190
BEA	12 MR	6.6 × 6.7 Å 5.6 × 5.6 Å	−42	156–159	198–201
FAU	12 MR	7.4 × 7.4 Å	−31	165	196

or that the acid strength of the materials is more similar than was assumed [39]. Our findings show that Si/Al ratios above Si/Al = 4.9 for MOR and Si/Al = 10.5 for Beta do not affect the acid strength of the Brønsted acid sites. We conclude that the differences in the heat of adsorption, and thus the size and shape of the pores, are the dominant factors in determining the cracking activity of the Brønsted acid sites [25,27,39]. The better the fit between pore and reactant, the higher the observed rate per Brønsted acid site of the reaction.

4.2. Structure of active site: dehydrogenation

The apparent activities of dehydrogenation varied with the zeolite structure type (Table 2), but no relationship with pore size was found. Increasing the Si/Al ratio of zeolites increased the apparent activation energy. Monomolecular dehydrogenation proceeded via protonation on a C–H bond, followed by the release of hydrogen and formation of alkoxide species that desorb as olefins (Scheme 1) [6,17,40]. The rate-limiting step of monomolecular dehydrogenation differs from that of cracking. Theoretical calculations predict that a hydrogen molecule and an alkoxide species are formed in the transition state of dehydrogenation [9,10]. Hydrogen is desorbed, and an alkoxide species is formed. The structure, and thus the stability, of this transition state strongly resemble those of the alkoxide. Biscardi and Iglesia [41] and Yu et al. [42] suggested that the predominant role of extra-framework cations like Zn and Co in Zn/H-ZSM5 and Co/H-ZSM5 is to enhance the recombinative desorption of hydrogen, which increases the rate of dehydrogenation compared to H-ZSM5. Kazansky et al. [43] showed experimentally that the role of Zn cations on Zn-ZSM5 is the dissociative adsorption of hydrocarbon, forming an alkyl group and a Brønsted acid site, which differs from the theoretically predicted mechanism over H-ZSM5. Narbeshuber et al. [13] showed a dependence of the hydrocarbon chain length and the amount of branching on the rates and apparent activation energies in dehydrogenation of hydrocarbons over H-ZSM5. Thus, in H-ZSM5, hydrocarbon species are involved in the rate-limiting step, in contrast to Zn/H-ZSM5 and Co/H-ZSM5, in which the rate-limiting step may involve formation of hydrogen. The presence of only a very small isotope effect in a steady-state isotope transient (n-H_{10}-butane to n-D_{10}-butane) experiment suggests that desorption of olefin is the rate-limiting step [13]. Thus, the stability of alkoxide species determines the apparent activity of dehydrogenation, and the reaction does not depend on the acid strength of the Brønsted acid sites to the same extent as cracking.

A quantum chemical study on the stability of C_3–C_5 alkoxide species, reported by Nieminen et al. [24], showed that the chemisorption energies of olefins differ by almost 150 kJ/mol. Moreover, the stability of the alkoxides increases with chain length (−137, −156, and −198 kJ/mol for C_3, C_4, and C_5, respectively), which is in good agreement with experimental results of Narbeshuber et al. [13], who reported that the apparent activation energy of monomolecular dehydrogenation increased with carbon number, 95 (C_3), 115 (C_4), and 150 (C_5) kJ/mol over H-ZSM5. Theory also predicted that a hindered local geometry around the active site of the zeolite has a destabilizing effect on the bulkier alkoxide species. Other theoretical calculations indicated that the alkoxide species interacts covalently with zeolites and is further stabilized by van der Waals interaction with the zeolite framework, and that the nearby framework oxygens of the Brønsted acid sites also play a role in stabilization [44–46]. This means that not only the Brønsted acid sites, but also the region surrounding the sites, participate in the reaction. Thus, changes in zeolite structure and such properties as the Si/Al ratio, framework ionicity, and framework flexibility strongly influence the stability of the alkoxide species.

Other reactions that involve alkoxide species may be similarly dependent on the stability of these species. One such reaction is alkylation, in which hydride transfer from an alkane to an alkoxide largely determines the product distribution over the catalyst. Various authors have reported that high rates of hydride transfer and stable alkylation catalysts require a high Brønsted acid site density [47,48]. Sanchez-Castillo et al. [47] showed that the activation energy is lower for zeolites with higher Brønsted acid site density, similar to our observation for the dehydrogenation reaction, which may suggest that this reaction also depends on the stability of alkoxide species involved in the reaction. Another study [48] found that the rate of hydride transfer was slowed by a higher Si/Al ratio of zeolite Beta compared with Y and that a high Brønsted acid site density caused high hydride transfer and favored a long catalyst life. This is in line with the results of catalytic cracking experiments in which lower framework Si/Al ratios gave higher hydride transfer rates [49].

5. Conclusion

Different reactions depend differently on the strength and local structure of the Brønsted acid sites in zeolites. The activity of Brønsted acid sites in zeolites is strongly affected by the rate-limiting step of the reaction. The monomolecular cracking of alkanes proceeds via protonation of the alkane as the rate-limiting step. This reaction is affected by the size and shape of the pores that affect the heat of adsorption; the intrinsic reaction parameters are much more similar than the apparent values, which are not corrected for the heat of adsorption. The rate-limiting step in dehydrogenation of alkanes is desorption of the alkoxide species, and the rate is determined by the stability of the alkoxide species. This stability depends on the local struc-

ture of the Brønsted acid site and the Si/Al ratio of the zeolite framework.

Acknowledgments

The authors thank Anuji Abraham for assisting with the ^{27}Al MAS NMR measurements and Hye Ja Jung for preparing the Beta samples.

References

[1] J. Ward, J. Catal. 11 (1968) 259.
[2] J. Abott, F.N. Guerzoni, Appl. Catal. 85 (1992) 173.
[3] W.O. Haag, R.M. Dessau, in: Proceedings, 8th International Congress on Catalysis Berlin, 1984, vol. 2, Dechema, Frankfurt-am-Main, 1984, p. 305.
[4] A. Corma, J. Planelles, J. Sanchez-Marin, F. Thomas, J. Catal. 93 (1985) 30.
[5] A.F.H. Wielers, M. Vaarkamp, M.F.M. Post, J. Catal. 127 (1991) 51.
[6] A.G. Olah, Y. Halpern, J. Shen, K.Y. Mo, J. Am. Chem. Soc. 95 (1973) 4960.
[7] W.O. Haag, R.M. Lago, P.B. Weisz, Faraday Discuss. Chem. Soc. 72 (1981) 317.
[8] J.A. Lercher, R.A. van Santen, H. Vinek, Catal. Lett. 27 (1994) 91.
[9] V.B. Kazansky, I.W. Senchenya, J. Catal. 119 (1989) 108.
[10] V.B. Kazansky, M.V. Frash, R.A. van Santen, Catal. Lett. 28 (1994) 211.
[11] W.O. Haag, R.M. Dessau, R.M. Lago, Stud. Surf. Sci. Catal. 60 (1991) 255.
[12] T.F. Narbeshuber, H. Vinek, J.A. Lercher, J. Catal. 157 (1995) 388.
[13] T.F. Narbeshuber, A. Brait, K. Seshan, J.A. Lercher, J. Catal. 172 (1997) 127.
[14] M.T. Aronson, R.J. Gorte, W.E. Farneth, D. White, J. Am. Chem. Soc. 111 (1989) 840.
[15] J.F. Haw, B.R. Richardson, B.R. Oshiro, N.D. Lazo, J.A. Speed, J. Am. Chem. Soc. 111 (1989) 2052.
[16] V.B. Kazansky, Catal. Today 51 (1999) 419.
[17] V.B. Kazansky, Acc. Chem. Res. 24 (1991) 379.
[18] A. Corma, Curr. Opin. Solid State Mater. Sci. 2 (1997) 63.
[19] A. Bhan, Y.V. Joshi, W.N. Delgass, K.T. Thomson, J. Phys. Chem. B 107 (2003) 10476.
[20] J.A. van Bokhoven, A.M.J. van der Eerden, R. Prins, J. Am. Chem. Soc. 126 (2004) 4506.
[21] J.A. Lercher, K. Seshan, Curr. Opin. Solid State Mater. Sci. 2 (1997) 57.
[22] A. Auroux, A. Tuel, J. Bandiera, B.Y. Taarit, Appl. Catal. 93 (1993) 181.
[23] M. Temkin, Adv. Catal. 28 (1979) 173.
[24] V. Nieminen, M. Sierka, D.Y. Murzin, J. Sauer, J. Catal. 231 (2005) 393.
[25] S.M. Babitz, B.A. Williams, J.T. Miller, R.Q. Snurr, W.O. Haag, H.H. Kung, Appl. Catal. A 179 (1999) 71.
[26] S. Kotrel, M.P. Rosynek, J.H. Lunsford, J. Phys. Chem. B 103 (1999) 818.
[27] J.A. van Bokhoven, B.A. Williams, W. Ji, D.C. Koningsberger, H.H. Kung, J.T. Miller, J. Catal. 224 (2004) 50.
[28] I. Yuranov, D.A. Bulushev, A. Renken, L. Kiwi-Minsker, J. Catal. 227 (2004) 138.
[29] A. Abraham, S.H. Lee, C.H. Shin, S.B. Hong, R. Prins, J.A. van Bokhoven, Phys. Chem. Chem. Phys. 6 (2004) 3031.
[30] T.J.G. Kofke, R.J. Gorte, W.E. Farneth, J. Catal. 114 (1988) 34.
[31] P.A. Jacobs, H.E. Leeman, J.B. Uytterhoeven, J. Catal. 33 (1974) 17, 31.
[32] W.O. Haag, R.M. Lago, P.B. Weisz, Nature 309 (1984) 589.
[33] J. Engelhardt, W.K. Hall, J. Catal. 125 (1990) 472.
[34] S.M. Babitz, M.A. Kuehne, H.H. Kung, J.T. Miller, Ind. Eng. Chem. Res. 36 (1997) 3027.
[35] A.I. Biaglow, D.J. Parrillo, R.J. Gorte, J. Catal. 144 (1993) 193.
[36] S. Kotrel, M.P. Rosynek, J.H. Lunsford, J. Catal. 182 (1999) 278.
[37] F. Eder, M. Stockenhuber, J.A. Lercher, J. Phys. Chem. B 101 (1997) 5414.
[38] T.L.M. Maesen, E. Beerdsen, S. Calero, D. Dubbeldam, B. Smit, J. Catal. 237 (2006) 278.
[39] C.E. Ramachandran, B.A. Williams, J.A. van Bokhoven, J.T. Miller, J. Catal. 233 (2005) 100.
[40] H. Krannila, W.O. Haag, B.C. Gates, J. Catal. 135 (1992) 115.
[41] J.A. Biscardi, E. Iglesia, J. Catal. 182 (1999) 117.
[42] S.Y. Yu, G.J. Yu, W. Li, E. Iglesia, J. Phys. Chem. B 106 (2002) 4714.
[43] V.B. Kazansky, I.R. Subbotina, N. Rane, R.A. van Santen, E.J.M. Hensen, Phys. Chem. Chem. Phys. 7 (2005) 3088.
[44] R.S. Blaszkowski, R.A. van Santen, Top. Catal. 4 (1997) 145.
[45] X. Rozanska, Th. Demuth, F. Hutschka, J. Hafner, R.A. van Santen, J. Phys. Chem. B 106 (2002) 3248.
[46] X. Rozanska, R.A. van Santen, Th. Demuth, F. Hutschka, J. Hafner, J. Phys. Chem. B 107 (2003) 1309.
[47] M.A. Sanchez-Castillo, R.J. Madon, J.A. Dumesic, J. Phys. Chem. B 109 (2005) 2164.
[48] A. Feller, A. Guzman, I. Zuazo, J.A. Lercher, J. Catal. 224 (2004) 80.
[49] K.A. Cumming, B.W. Wojciechowski, Catal. Rev.-Sci. Eng. 38 (1996) 101.